

# The neutron and proton mass radii from vector meson photoproduction data on deuterium target

Chengdong Han,<sup>1,2</sup> Gang Xie,<sup>1,3</sup> Wei Kou,<sup>1,2</sup> Rong Wang,<sup>1,2,\*</sup> and Xurong Chen<sup>1,2,3,†</sup>

<sup>1</sup>*Institute of Modern Physics, Chinese Academy of Sciences, Lanzhou 730000, China*

<sup>2</sup>*University of Chinese Academy of Sciences, Beijing 100049, China*

<sup>3</sup>*Guangdong Provincial Key Laboratory of Nuclear Science, Institute of Quantum Matter, South China Normal University, Guangzhou 510006, China*

(Dated: January 24, 2022)

Tremendous progresses have been achieved for the proton structure and radius measurements, but not so many for the neutron. In this paper, we extract the mass radii of the neutron and the proton from the analysis of the differential cross sections of near-threshold  $\omega$  and  $\phi$  photoproductions on deuterium target, which is regarded as a quasi-free neutron plus a quasi-free proton. The incoherent data of  $\omega$  and  $\phi$  photoproductions are provided by CBELSA/TAPS collaboration and LEPS collaboration respectively, where the deuteron is disintegrated in the experiments to measure the properties of the individual nucleons. With the near-threshold data of  $\gamma d \rightarrow \omega n(p)$  and  $\gamma d \rightarrow \omega p(n)$ , the neutron and proton mass radii are determined to be  $0.795 \pm 0.092$  fm and  $0.741 \pm 0.028$  fm respectively. With the near-threshold and incoherent  $\phi$  photoproduction data of  $\gamma d \rightarrow \phi pn$ , the average mass radius of the bound nucleon (neutron or proton) inside the deuteron is extracted to be  $0.752 \pm 0.039$  fm. For a comparison study, we also extract the mass radius of the free proton from the exclusive and inclusive  $\omega$  photoproductions on the hydrogen target by the CBELSA/TAPS collaboration. From our analysis, we find that the neutron mass radius is close to the proton mass radius with no obvious difference, and the nuclear modification on the mass radius is not significant inside the deuteron.

## I. INTRODUCTION

Understanding the structure of matter has been deep into the interior of the nucleon: quarks and gluons. In the modern physical picture, the nucleon is often described as a “bag” full of quarks, antiquarks and gluons, which is the most abundant and the stable quantum chromodynamics (QCD) bound state in nature. The study of the nucleon structure is one important aspect to understand the strong interaction force. But as the physicists gradually deepen their understanding on the internal structure of the nucleon, more and more puzzles have been arisen as well. For example, what are the origins of the proton mass? The sum of the masses of the valence quarks only accounts for about one percent of the proton mass. Most of the mass of the proton comes from the self-interactions of gluons, but we lack a more specific understanding of this part. The mass distribution inside the hadron is one important feature of the particular hadron. Extracting the proton and neutron mass distributions is of significance for the study of the equations of state of the dense nuclear matter, such as the neutron star. In all, understanding the proton mass problem theoretically and experimentally is a hot topic in the field of high-energy nuclear physics in recent years [1–11].

For exploring the mass structure and mechanical properties of the proton, the graviton would be an useful probe. In principle, we can study the mass distribution in

the proton by exploiting the scattering between a graviton and the proton. But in fact, gravity is dozens of orders of magnitude weaker than the electromagnetic force, making the interaction between the graviton and the proton far exceeding the current limit of any experimental techniques [12]. Moreover, due to the color confinement effect of the strong interaction, the scattering between the bound quark-gluon system and the graviton is difficult to calculate directly. Hence we should look for a realistic way to detect the mass structure of the proton.

In astrophysics and cosmology, the study of the distribution of mass in galaxies gave birth to the hypothesis of the presence of dark matter in the Universe. Similarly, for the proton, the charged lepton scattering experiments revealed the spatial distribution of the quarks (“visible” to photons), but do not directly probe the spatial distribution of the gluons (“invisible” to photons). Gluons play an important role for the proton mass generation [3, 9, 10]. Therefore, to probe the mass distribution inside the proton, we need to think of a new probe other than the photon.

A more feasible way to probe the nucleon mass distribution is to utilize the elastic scattering between a heavy quarkonium and the hydrogen (deuterium) targets [13–15]. The possible method is to convert the study of graviton-proton scattering into a scalar gravitational form factor (GFF) of the proton, under the theoretical framework of the vector-meson-dominance model [15]. As we focus on the neutron mass radius in this work, Fig. 1 shows the diagram of the scattering between a dipole and the neutron. According to a low-energy theorem, this process of a quarkonium production (vector meson) is sensitive to the scalar GFF and so to measure

\* rwang@impcas.ac.cn

† xchen@impcas.ac.cn

the mass distribution inside the neutron.

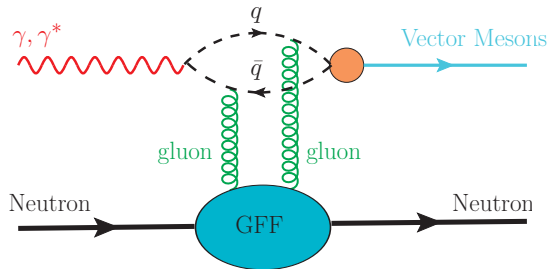


FIG. 1. The Feynman diagram of the scattering between the quark-antiquark pair and the neutron for the near-threshold vector meson photoproductions. The form factor of the energy-momentum tensor is detected with the two-gluon exchange process.

In the weak-field approximation, the scalar GFF can be used to describe the mass distribution of nucleon [15]. Specifically, the mass radius  $\langle R_m^2 \rangle$  is defined as the derivative of GFF with zero momentum transfer to the nucleon, which is given by

$$\langle R_m^2 \rangle \equiv \frac{6}{M} \frac{dG(t)}{dt} \Big|_{t=0}, \quad (1)$$

where the scalar GFF is normalized to  $M$  at zero momentum transfer ( $G(0) = M$ ). This definition is similar to the charge radius, which is valid to estimate the root-mean-square radius in the process of low-momentum exchange.

The scalar GFF is defined as the form factor of the trace of the QCD energy-momentum tensor (EMT) [3, 4, 15]. And the scalar GFF is usually parameterized as the dipole form  $G(t) = M/(1 - t/m_s^2)^2$ , and  $m_s$  is a free parameter to be determined by the experimental data. The differential cross section of quarkonium photoproduction near the threshold is directly related to the matrix element of the scalar gluon operator, thus the scalar GFF can be accessed with the process [15, 16]. In the small momentum transfer region, the differential cross section of the quarkonium photoproduction near threshold can be described with the scalar GFF, which is written as the following formalism [15, 17, 18],

$$\frac{d\sigma}{dt} \propto G^2(t). \quad (2)$$

By analysing the differential cross section of vector meson photoproduction near threshold on the nucleon target, we could extract the dipole-size parameter  $m_s$  of the scalar form factor. Then we can obtain the mass radius information by using Eq. (1).

As the proton mass radius has already been fixed by the data of  $\omega$ ,  $\phi$ , and  $J/\psi$  vector meson photoproductions near threshold in the previous analysis [15, 17, 18], we would like to see whether the neutron mass radius can be extracted in experiment as well. The recent time-like measurement of neutron shows that the effective form

factor of neutron has the different oscillation behavior compared to that of proton [19]. It is interesting to see whether or not the mass distribution and mass radius of the neutron are different from those of the proton. To study the neutron mass radius, we could use the deuterium target data, in which the neutron and the proton are loosely bound. Therefore we turn to the incoherent photoproduction of vector mesons where the neutron or the proton is knocked out.

## II. DATA ANALYSES OF VECTOR MESON PHOTOPRODUCTIONS NEAR THRESHOLD

The vector-meson-dominance (VMD) model is quite successful in describing the light vector meson photoproductions. Therefore it provides a valuable method to study the quarkonium-nucleon scattering, so as to probe the nucleon mass radius within the theoretical framework of operator product expansion and low-energy theorems. Following our previous works assuming a dipole form GFF to extract the proton and deuteron mass radii from near-threshold vector meson photoproductions [17, 18], we perform a series of analyses of the neutron and proton mass radii from the differential cross section data of vector meson photoproductions near thresholds on the deuterium target, including the experimental data of  $\omega$  and  $\phi$  vector mesons [20, 21].

### A. Mass radius of quasi-free neutron with $\omega$ meson probe

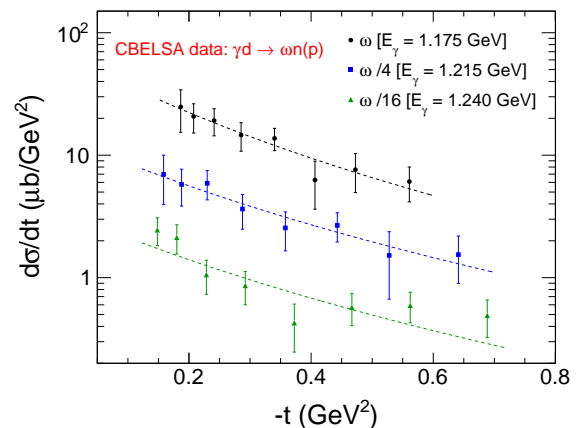


FIG. 2. Differential cross sections of the near-threshold photoproduction of  $\omega$  meson as a function of the momentum transfer  $-t$  off the quasi-free neutron in the deuterium target [20]. The three incident photon energies ( $E_\gamma = 1.175, 1.215$  and  $1.240$  GeV) near the threshold of  $\omega$  meson production are labeled in the figure. Some cross sections are scaled using the coefficients indicated in the figure, to avoid the overlapping of the data points.

TABLE I. The extracted values of the dipole-size parameter  $m_s$  and the quasi-free neutron mass radii  $R_m^{n*}$  from the differential cross-section data of near-threshold  $\omega$  productions off the bound neutron in deuterium at different incident photon energies.

$E_\gamma$ (GeV)	1.175	1.215	1.240
$m_s$ (GeV)	$0.799 \pm 0.145$	$0.893 \pm 0.179$	$0.900 \pm 0.200$
$\sqrt{\langle R_m^2 \rangle}$ (fm)	$0.855 \pm 0.155$	$0.765 \pm 0.153$	$0.759 \pm 0.169$

Fig. 2 shows the differential cross section of the  $\omega$  meson produced on the bound neutron as a function of the momentum transfer  $-t$ , at different photon energies near the threshold. For the measurement of this reaction at ELSA [20], exactly four neutral hits are identified (three photons from the decay of  $\omega$  and one neutron that struck out from deuteron), to make sure the  $\omega$  meson was produced on the bound neutron in the liquid deuterium target and the exclusivity ( $\gamma d \rightarrow \omega n(p)$ ). The  $t$ -dependence of the differential cross sections are fitted with the scalar GFF  $G(t)$  of the dipole parametrization. We determined the dipole parameter  $m_s$  and the quasi-free neutron mass radius  $R_m^{n*}$  from the model fitting to the deuterium data [20] at three different incident photon energies ( $E_\gamma = 1.175, 1.215, 1.240$  GeV). The obtained dipole parameter  $m_s$  and the quasi-free neutron mass radii  $R_m^{n*}$  at different near-threshold energies are listed in Table I. The average quasi-free neutron mass radius of the three extracted values at different energies is calculated to be  $0.795 \pm 0.092$  fm.

### B. Mass radius of quasi-free proton with $\omega$ meson probe

TABLE II. The extracted values of the dipole-size parameter  $m_s$  and the quasi-free proton mass radii  $R_m^{p*}$  from the differential cross-section data of near-threshold  $\omega$  productions off the bound proton in deuterium at different incident photon energies.

$E_\gamma$ (GeV)	1.175	1.215	1.240
$m_s$ (GeV)	$0.863 \pm 0.056$	$1.035 \pm 0.076$	$0.881 \pm 0.055$
$\sqrt{\langle R_m^2 \rangle}$ (fm)	$0.792 \pm 0.051$	$0.660 \pm 0.048$	$0.776 \pm 0.048$

Fig. 3 shows the differential cross section of the  $\omega$  meson produced on the bound proton as a function of the momentum transfer  $-t$ , at different photon energies near the threshold. For the measurement of this reaction at ELSA [20], exactly three neutral hits and one charged hit are identified (three photons from the decay of  $\omega$  and one proton that struck out from deuteron), to make sure the  $\omega$  meson was produced on the bound proton in the liquid deuterium target and the exclusivity ( $\gamma d \rightarrow \omega p(n)$ ). The

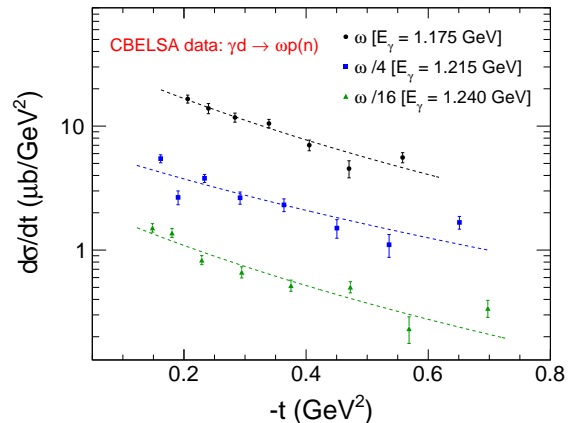


FIG. 3. Differential cross sections of the near-threshold photoproduction of  $\omega$  meson as a function of the momentum transfer  $-t$  off the quasi-free proton in the deuterium target [20]. The three incident photon energies ( $E_\gamma = 1.175, 1.215$  and  $1.240$  GeV) near the threshold of  $\omega$  meson production are labeled in the figure. Some cross sections are scaled using the coefficients indicated in the figure, to avoid the overlapping of the data points.

$t$ -dependence of the differential cross sections are fitted with the scalar GFF  $G(t)$  of the dipole parametrization. We determined the dipole parameter  $m_s$  and the quasi-free proton mass radius  $R_m^{p*}$  from the model fitting to the deuterium data [20] at three different incident photon energies ( $E_\gamma = 1.175, 1.215, 1.240$  GeV). The obtained dipole parameter  $m_s$  and the quasi-free proton mass radii  $R_m^{p*}$  at different near-threshold energies are listed in Table II. The average quasi-free proton mass radius of the three extracted values at different energies is calculated to be  $0.741 \pm 0.028$  fm. We see that the mass radii of the loosely bound proton and loosely bound neutron inside the deuteron are of no big difference.

### C. Mass radius of free proton with $\omega$ meson probe

Fig. 4 and Fig. 5 show respectively the exclusive and the inclusive cross-section data of near-threshold  $\omega$  meson photoproduction off the free proton in liquid hydrogen target [20]. The differential cross sections are shown as a function of momentum transfer  $-t$ . For the exclusive data, the recoil nucleon was detected in coincidence. For the inclusive data, no condition is placed for the detection of the knock-out nucleon. The  $t$ -dependence of the differential cross sections are fitted with the scalar GFF  $G(t)$  of the dipole parametrization. We determined the dipole parameter  $m_s$  and the free proton mass radius  $R_m^p$  from the model fitting to the hydrogen data [20] at four different incident photon energies ( $E_\gamma = 1.138, 1.625, 1.188, 1.225$  GeV). The obtained dipole parameter  $m_s$  and the free proton mass

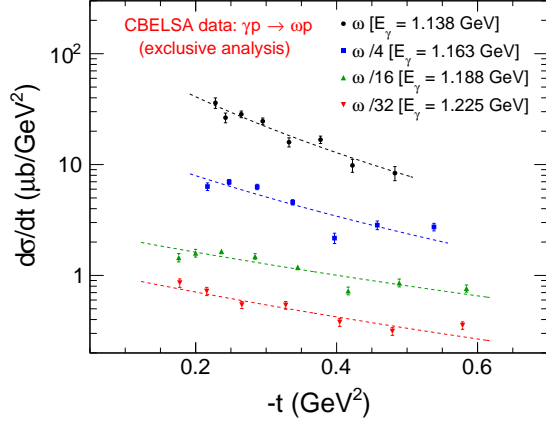


FIG. 4. Differential cross sections of the near-threshold photoproduction of  $\omega$  meson as a function of the momentum transfer  $-t$  off the free proton in the hydrogen target [20]. The four incident photon energies ( $E_\gamma = 1.138, 1.163, 1.188$  and  $1.225$  GeV) near the threshold of  $\omega$  meson production are labeled in the figure. The exclusive data by CBELSA/TAPS Collaboration are used, where the recoil proton is identified. Some cross sections are scaled using the coefficients indicated in the figure, to avoid the overlapping of the data points.

radii  $R_m^p$  at different near-threshold energies from the exclusive analysis and the inclusive analysis are listed in Table III and Table IV, respectively. The average free proton mass radius of the exclusive analysis and the inclusive analysis are  $0.654 \pm 0.023$  fm and  $0.649 \pm 0.025$  fm, respectively, with the near-threshold  $\omega$  production data by CBELSA/TAPS Collaboration [20]. We see that the mass radii of the free proton based on the exclusive data and the inclusive data are very close to each other. We also see that the free proton mass radius may be different from the bound proton mass radius in deuteron, but more precise data are needed to confirm this finding.

#### D. The nucleon mass radius with $\phi$ meson probe

In the following analysis, the nucleon mass radius refers to the averaged value of the proton mass radius and the neutron mass radius. From the analyses in above sections, we have obtained the mass radii of the quasi-free neutron, the quasi-free proton and the free proton, with the  $\omega$  meson probe. And the mass radii of the quasi-free neutron and the quasi-free proton are quite close. In this section, we would like to check these findings with the measurements of the  $\phi$  meson probe. It is interesting and necessary to look at the probe-dependence for the neutron mass radius and the proton mass radius.

Fig. 6 shows the differential cross section of the  $\phi$  meson produced on the bound nucleon as a function of the momentum transfer  $-t$ , at different photon energies near the production threshold [21]. For the used inco-

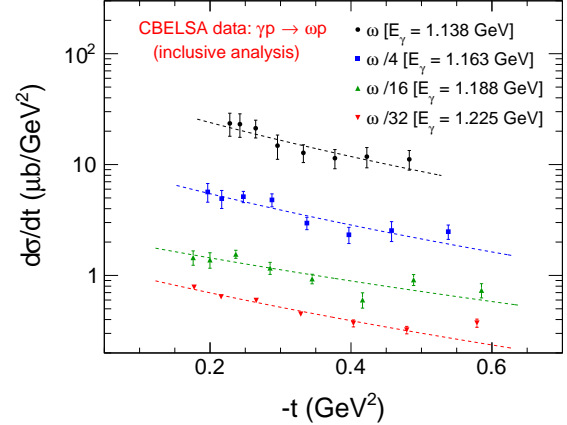


FIG. 5. Differential cross sections of the near-threshold photoproduction of  $\omega$  meson as a function of the momentum transfer  $-t$  off the free proton in the hydrogen target [20]. The four incident photon energies ( $E_\gamma = 1.138, 1.163, 1.188$  and  $1.225$  GeV) near the threshold of  $\omega$  meson production are labeled in the figure. The inclusive data by CBELSA/TAPS Collaboration are used, where no requirement is made for the recoil proton detected in coincidence. Some cross sections are scaled using the coefficients indicated in the figure, to avoid the overlapping of the data points.

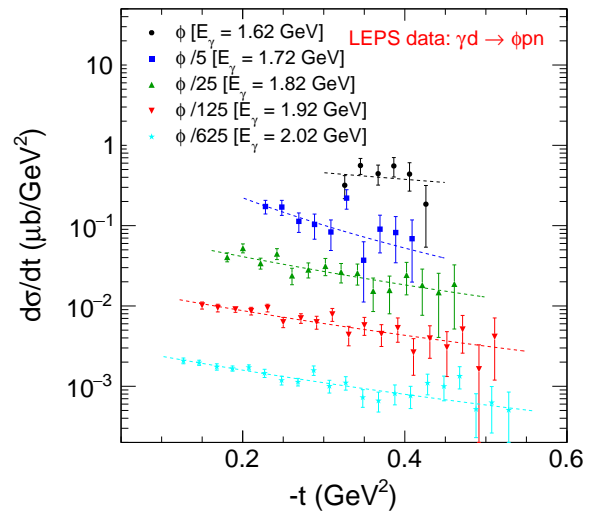


FIG. 6. Differential cross sections of the incoherent and near-threshold photoproduction of  $\phi$  meson as a function of the momentum transfer  $-t$  off the quasi-free nucleon in the deuterium target ( $\gamma d \rightarrow \phi p n$ ) [21]. The five incident photon energies ( $E_\gamma = 1.62, 1.72, 1.82, 1.92$  and  $2.02$  GeV) near the threshold of  $\phi$  meson production are labeled in the figure. Some cross sections are scaled using the coefficients indicated in the figure, to avoid the overlapping of the data points.

herent data on the deuterium target at LEPS [21], they are selected with a cut on the missing mass spectra, to make sure the  $\phi$  meson was interacting with the individual nucleon instead of the whole deuteron. The  $t$ -dependence of the differential cross sections are fitted with the scalar GFF  $G(t)$  of the dipole parametrization. We determined the dipole parameter  $m_s$  and the quasi-free nucleon mass radius  $R_m^{N^*}$  from the model fitting to the deuterium data [21] at five different incident photon energies ( $E_\gamma = 1.62, 1.72, 1.82, 1.92, 2.02$  GeV). The obtained dipole parameter  $m_s$  and the quasi-free nucleon mass radii  $R_m^{N^*}$  at different near-threshold energies are listed in Table V. The average quasi-free nucleon mass radius of the five extracted values at different energies is calculated to be  $0.752 \pm 0.039$  fm, with the  $\phi$  meson probe. This quasi-free nucleon mass radius is just between the mass radii of the quasi-free neutron and the quasi-free proton probed with the  $\omega$  meson probe. We see that the mass radii of the quasi-free neutron, the quasi-free proton, and the quasi-free nucleon are consistent with each other. The other finding is that the dependence on the meson probe is weak for the mass radius measurement, in terms of the analyses of the  $\omega$  meson data and the  $\phi$  meson data.

### III. DISCUSSIONS AND SUMMARY

Based on the extracted mass radii of the bound neutron in deuteron, the bound proton in deuteron, and the free proton, we calculated the ratios among them. In Table VI, we list the ratio of the bound neutron mass radius to the bound proton mass radius, the ratio of the bound proton mass radius in deuteron to the free proton mass radius, and the ratio of the bound neutron mass radius in deuteron to the free proton mass radius. We find that the obtained quasi-free neutron mass radius is about  $7.3 \pm 13.0\%$  larger than the obtained quasi-free proton mass radius. The obtained bound proton mass radius in deuteron is about  $13.8 \pm 6.1\%$  larger than the free proton mass radius. To conclude, first, the neutron mass radius is of no significant difference to the proton mass radius, with the current precision of the experiment. This is within our expectations, since isospin symmetry is a rather good symmetry. Second, the mass radius of the bound nucleon may be a little bit larger than that of the free nucleon. This result is actually in consistence with

the popular “nucleon swelling” picture for the explanation of nuclear medium modifications on parton distribution functions [22–25]. The “nucleon swelling” in nucleus can be understood as the six-quark bag configuration or the gluon exchanges between the nucleons. Our analysis result hints that the gluon distribution inside the bound nucleon is different from that inside the free nucleon.

The near-threshold photoproduction of a vector meson on the neutron or the proton can be well described with the scalar GFF of dipole form. Within this model, we determined the neutron mass radius in deuteron to be  $0.795 \pm 0.092$  fm from the data of  $\omega$  photoproductions near the threshold energies. We also determined the nucleon mass radius in deuteron to be  $0.752 \pm 0.039$  fm from the incoherent  $\phi$  photoproduction data on the deuterium target ( $\gamma d \rightarrow \phi pn$ ). The obtained neutron and proton mass radii are consistent with the obtained nucleon mass radius. Similar to the proton, the neutron mass radius is smaller than the neutron magnetic radius. The possible explanation is that the mass distribution mainly counts on the gluon fluctuations and the electric current distribution mainly counts on the quarks.

At present, the Electron-ion collider in China (EicC) [26–28] and the Electron-Ion Collider in the USA (EIC) [29, 30] are proposed, which will provide good opportunities to study the near-threshold heavy quarkonia photoproductions on the proton or the nucleus target by exploiting the abundant virtual photon flux at low  $Q^2$ . These heavy vector meson photoproduction experiments at EicC and EIC will further test the VMD model and the scalar GFF assumptions used in this work. The future experiments on electron-ion colliders will enhance our understanding on the nucleon mass distribution and radius, which are preliminarily studied and discussed with the current light quarkonium data. The study of the mass structure of the nucleon surely will advance our understandings on the nonperturbative features of QCD, the origins of proton mass, and the color confinement mechanism of the strong interaction.

### ACKNOWLEDGMENTS

This work is supported by the Strategic Priority Research Program of Chinese Academy of Sciences under the Grant NO. XDB34030301 and the National Natural Science Foundation of China under the Grant NO. 12005266.

- 
- [1] X.-D. Ji, Phys. Rev. Lett. **74**, 1071 (1995), arXiv:hep-ph/9410274.
  - [2] X.-D. Ji, Phys. Rev. D **52**, 271 (1995), arXiv:hep-ph/9502213.
  - [3] X. Ji and Y. Liu, Sci. China Phys. Mech. Astron. **64**, 281012 (2021), arXiv:2101.04483 [hep-ph].
  - [4] X. Ji, Front. Phys. (Beijing) **16**, 64601 (2021), arXiv:2102.07830 [hep-ph].
  - [5] C. Lorcé, Eur. Phys. J. C **78**, 120 (2018), arXiv:1706.05853 [hep-ph].
  - [6] C. Lorcé, A. Metz, B. Pasquini, and S. Rodini, JHEP **11**, 121 (2021), arXiv:2109.11785 [hep-ph].
  - [7] A. Metz, B. Pasquini, and S. Rodini, Phys. Rev. D **102**, 114042 (2020), arXiv:2006.11171 [hep-ph].

- [8] K.-F. Liu, Phys. Rev. D **104**, 076010 (2021), arXiv:2103.15768 [hep-ph].
- [9] Y.-B. Yang, J. Liang, Y.-J. Bi, Y. Chen, T. Draper, K.-F. Liu, and Z. Liu, Phys. Rev. Lett. **121**, 212001 (2018), arXiv:1808.08677 [hep-lat].
- [10] F. He, P. Sun, and Y.-B. Yang ( $\chi$ QCD), Phys. Rev. D **104**, 074507 (2021), arXiv:2101.04942 [hep-lat].
- [11] R. Wang, J. Evslin, and X. Chen, Eur. Phys. J. C **80**, 507 (2020), arXiv:1912.12040 [hep-ph].
- [12] H. Pagels, Phys. Rev. **144**, 1250 (1966).
- [13] D. Kharzeev, Proc. Int. Sch. Phys. Fermi **130**, 105 (1996), arXiv:nucl-th/9601029.
- [14] D. Kharzeev, H. Satz, A. Syamtomov, and G. Zinovjev, Eur. Phys. J. C **9**, 459 (1999), arXiv:hep-ph/9901375.
- [15] D. E. Kharzeev, Phys. Rev. D **104**, 054015 (2021), arXiv:2102.00110 [hep-ph].
- [16] H. Fujii and D. Kharzeev, Phys. Rev. D **60**, 114039 (1999), arXiv:hep-ph/9903495.
- [17] R. Wang, W. Kou, Y.-P. Xie, and X. Chen, Phys. Rev. D **103**, L091501 (2021), arXiv:2102.01610 [hep-ph].
- [18] R. Wang, W. Kou, C. Han, J. Evslin, and X. Chen, Phys. Rev. D **104**, 074033 (2021), arXiv:2108.03550 [hep-ph].
- [19] M. Ablikim *et al.* (BESIII), Nature Phys. **17**, 1200 (2021).
- [20] F. Dietz *et al.* (CBELSA/TAPS), Eur. Phys. J. A **51**, 6 (2015).
- [21] W. C. Chang *et al.* (LEPS), Phys. Lett. B **684**, 6 (2010), arXiv:0907.1705 [nucl-ex].
- [22] F. E. Close, R. G. Roberts, and G. G. Ross, Phys. Lett. B **129**, 346 (1983).
- [23] R. L. Jaffe, Phys. Rev. Lett. **50**, 228 (1983).
- [24] R. Wang, R. Dupre, Y. Huang, B. Zhang, and S. Niccolai, Phys. Rev. C **99**, 035205 (2019), arXiv:1806.09148 [hep-ph].
- [25] G. A. Miller, Phys. Rev. Lett. **123**, 232003 (2019), arXiv:1907.00110 [nucl-th].
- [26] X. Chen, PoS **DIS2018**, 170 (2018), arXiv:1809.00448 [nucl-ex].
- [27] X. Chen, F.-K. Guo, C. D. Roberts, and R. Wang, Few Body Syst. **61**, 43 (2020), arXiv:2008.00102 [hep-ph].
- [28] D. P. Anderle *et al.*, Front. Phys. (Beijing) **16**, 64701 (2021), arXiv:2102.09222 [nucl-ex].
- [29] A. Accardi *et al.*, Eur. Phys. J. A **52**, 268 (2016), arXiv:1212.1701 [nucl-ex].
- [30] R. Abdul Khalek *et al.*, (2021), arXiv:2103.05419 [physics.ins-det].

TABLE III. The extracted values of the dipole-size parameter  $m_s$  and the free proton mass radii  $R_m^p$  from the differential cross-section data of near-threshold  $\omega$  productions off the free proton in hydrogen at different incident photon energies. The data are from the exclusive analysis.

$E_\gamma$ (GeV)	1.138	1.163	1.188	1.225
$m_s$ (GeV)	$0.627 \pm 0.049$	$0.809 \pm 0.076$	$1.171 \pm 0.064$	$1.118 \pm 0.076$
$\sqrt{\langle R_m^2 \rangle}$ (fm)	$1.090 \pm 0.084$	$0.845 \pm 0.079$	$0.584 \pm 0.032$	$0.611 \pm 0.042$

TABLE IV. The extracted values of the dipole-size parameter  $m_s$  and the free proton mass radii  $R_m^p$  from the differential cross-section data of near-threshold  $\omega$  productions off the free proton in hydrogen at different incident photon energies. The data are from the inclusive analysis.

$E_\gamma$ (GeV)	1.138	1.625	1.188	1.225
$m_s$ (GeV)	$0.914 \pm 0.207$	$0.966 \pm 0.128$	$1.172 \pm 0.127$	$1.042 \pm 0.044$
$\sqrt{\langle R_m^2 \rangle}$ (fm)	$0.748 \pm 0.169$	$0.708 \pm 0.094$	$0.583 \pm 0.063$	$0.656 \pm 0.028$

TABLE V. The extracted values of the dipole-size parameter  $m_s$  and the quasi-free nucleon mass radii  $R_m^{N*}$  from the differential cross-section data of incoherent and near-threshold  $\phi$  productions off the bound nucleon (proton or neutron) in deuterium at different incident photon energies.

$E_\gamma$ (GeV)	1.62	1.72	1.82	1.92	2.02
$m_s$ (GeV)	$1.326 \pm 1.436$	$0.511 \pm 0.189$	$0.831 \pm 0.128$	$0.914 \pm 0.085$	$0.926 \pm 0.064$
$\sqrt{\langle R_m^2 \rangle}$ (fm)	$0.515 \pm 0.558$	$1.338 \pm 0.495$	$0.823 \pm 0.127$	$0.748 \pm 0.069$	$0.738 \pm 0.051$

TABLE VI. The ratio of the quasi-free neutron mass radius  $R_m^{n*}$  to the quasi-free proton mass radius in the deuteron  $R_m^{p*}$ , the ratio of the quasi-free proton mass radius in the deuteron  $R_m^{p*}$  to the free proton mass radius  $R_m^p$ , and the ratio of the quasi-free neutron mass radius in the deuteron  $R_m^{n*}$  to the free proton mass radius  $R_m^p$ .

Category	$R_m^{n*}/R_m^{p*}$	$R_m^{p*}/R_m^p$	$R_m^{n*}/R_m^p$
Ratio	$1.073 \pm 0.130$	$1.133 \pm 0.059$	$1.142 \pm 0.062$